Effect of Mn Dopant on Structural and Optical Properties of $NiFe_2O_4$ Nanoparticles Synthesized by Autocombustion Method

M.B. SHELAR[1]*, K. M. PATIL[2], S. K. NALUGADE[2], V.R. CHAVAN[2], R.M. JADHAV[2], M.S.KORE[2] and A.V. GAIKWAD[2]

[1]Materials Research Laboratory, Department of Physics, D. Y. Patil College of Engineering and Technology (An Autonomous Institute), Kasaba Bawada, Kolhapur-416006, Maharashtra, India.
[2]Department of Chemical Engineering, D. Y. Patil College of Engineering and Technology (An Autonomous Institute), Kasaba Bawada, Kolhapur-416006, Maharashtra, India.

Abstract

The work is done on the Structural and optical properties of Manganese doped nickel nano ferrites prepared by auto route. The manganese is doped in nickel (Mn-Ni) mixed nano ferrites $Mn_xNi_{1-x}Fe_2O_4$ (x = 0.0, 0.2, 0.4, 0.6, 0.8, 1.0) have been synthesized by a simple auto combustion route. The cubic spinel structure were confined by using X- ray Diffraction for $Mn_xNi_{1-x}Fe_2O_4$ nano ferrite particles which shows favored positioning along with (311) direction. However, size of crystal increases from 20 nm to 26.38 nm increase in Mn content. The optical properties were examined by means of UV-visible absorption spectroscopy observed from 200 to 800 nm. Using the absorption spectra and Tauc's relation, the band gap was calculated and varies between 3.57 and 3.80 eV. The significant decline in the optical band gap was calculated with increasing manganese Composition from 3.80ev to 3.57 eV up to Mn=0.6, The further increase due to preparative crystallinity defects in composition from 3.67eV to 3.70 eV shows tunability of the optical band gap varying the concentration of Mn in nano ferrites. The present nanoparticles with variable narrow band gap may find applications in photocatalysis to increase the efficiency of photocatalytic reactions.

Introduction

Nano ferrite particles are recently finding potential applicant in automated industries due to their desirable optical and electrical properties.[1-2] Due to different properties of ferrites it has been prepared to meet the remarkable uses in microwave fields, engineering, permanent magnet, transformer core and memory chips etc. The spinel ferrites are semiconducting in nature. The electrical property depends on several factors including

the method of preparation, sintering temperature, sintering atmosphere, chemical composition and microstructure. as well as, by addition of impurities.[3] Ferrites containing Mn^{2+}ions tend to form α-Fe_2O_3 phase when heat treated above 200°C in air atmosphere.[4] It is very important to understand the mechanism involve in the change of properties. Nano ferrites are useful in types of biomedical fields such as X-ray diagnosis, drug delivery, hyperthermia, and magnetic resonance imaging (MRI).[5-8] Manganese ferrite ($MnFe_2O_4$) nanoparticles (NPs) with other ferrites are considered as a crucial tool for enhancing efficiency of magnetic resonance imaging, hyperthermia, and drug delivery.[9] Also, it is a mixed ferrite, where Mn^{2+} and Fe^{3+} occupies both tetrahedral and octahedral bonding sites.[10] The chemical changes in ferrites depend on their structural parameters of particle size and shape, which can be modified in the synthesis processes. In spinel ferrites, the physical and magnetic properties are powerfully reliant on cation distribution and process of research.[11, 12]

In the present work, the studies on $Mn_xNi_{1-x}Fe_2O_4$ (x = 0,0.2,0.4,0.6,0.8,1.0) ferrites annealed at 600 °C are reported. Powder X-ray diffraction (XRD), FT-IR spectroscopy techniques and spectrophotometer stayed active for structural and optical characterizations.

Material and Methods
Materials
For preparation of Mn doped Nickel nanoparticles, stoichiometric amounts of AR grade Manganese (II) Nitrates (Mn $(NO_3)_2$.$6H_2O$, (purity ~ 99%), AR grade Iron (III) Nitrates ($Fe(NO_3)_3$. $9H_2O$, (purity~ 98%) and AR grade Nickel (II) Nitrates ($Ni(NO_3)$. $6H_2O$), (purity ~ 99%) were used as starting materials and PVA (Polyvinyl Alcohol) and sucrose solutions from Merck, Mumbai were used as precipitating agent. Deionized water was used as solvent.

Sample Preparation
Manganese doped Nickel ferrite nanoparticles were prepared by self-propagating auto combustion route from a mixture of stoichiometric amount of (Mn $(NO_3)_2$. $6H_2O$, $Fe(NO_3)_3$. $9H_2O$ and Nickel Nitrates ($Ni(NO_3).6H_2O$). 10% of PVA and sucrose solutions were added it, where the sucrose is utilized for the combustion purpose and PVA forms the polymer resin with metal ions trapped in it. The whole

mixture was heated to about 80°C for the evolution of NO_2, CO_2, and H_2O. The mixture in solution transforms and converted to black fluffy gel. The PVA (the matrix) and Sucrose (the fuel) are dissolved together and at elevated temperature, and the brown fumed of solution gets evaporated. Sucrose provides the wrapping throughout the coordination for the cations in solution and circumvents their selective precipitation during the evaporation process. Black fluffy, and voluminous gel gets burnt in the self-propagating manner at about 90 °C. for 6 h to remove In order of residual water, the as-prepared Nickel ferrite nanoparticles was dried overnight and calcined at 600 °C. The prepared samples were used to study the structural and optical characterisation.

Characterization
Structural properties of the prepared $Mn_xNi_{1-x}Fe_2O_4$ (x = 0, 0.2, 0.4, 0.6, 0.8 and 1.0) nano ferrites were observed using the X-ray diffractometer (Rigaku Miniflex 600 with Cu $K\alpha_1$ radiation at 40 kV, 25 mA over the 2θ range of 10–100° (λ = 1.54056 Å). The optical properties of Nano powders were studied using the UV–Vis. Spectrophotometer (JASCO-V-770).
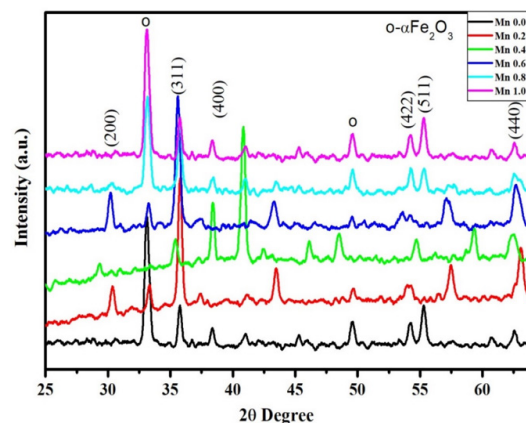
Fig.1: X ray diffraction patterns for $Mn_xNi_{1-x}Fe_2O_4$ ferrite (x = 0.2, 0.4, 0.6,0.8, 1.0) nanoparticles
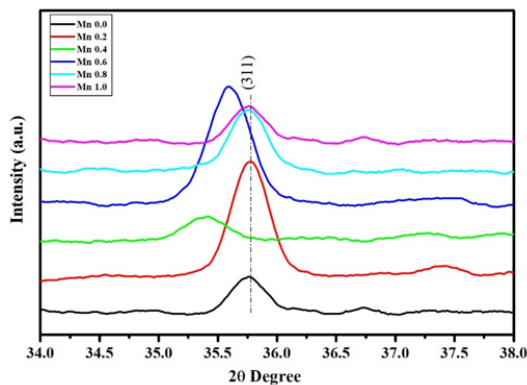
Results
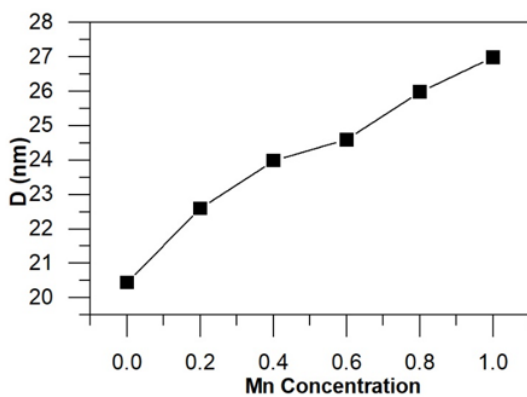### Result and Discussion
Structural Analysis
The XRD pattern of the prepared samples is shown in Fig 1 with noticeable (hkl) planes of (200), (311), (400), (422), (511), and (440) which are indexed with JCPDS card nos. 00-019-0629 for Fe_3O_4

and 00-010-0319 for $MnFe_2O_4$. The well-defined diffraction patterns confirm that the chemical reaction is completed. The observed diffraction peaks correspond to cubic spinel phase with the addition of some minor peaks as secondary phase (α-Fe_2O_3). The intensity of these peaks gently increases with an increase in the concentration of Mn^{2+} ion.

An enlarged view of the high-intensity characteristic peak (311) as shown in Fig.2. Manganese ions may have different ionic radius compared to nickel ions, leading to change in the lattice parameter of crystal structure, effect on spacing between lattice planes influencing the shift in position of (311) peak. It can induce strain in the crystal lattice, altering the diffraction pattern and casing peak shifts.[13]

The average crystallite size of the resulting powder materials, calculated using the Debye-Scherrer formula (equation 1), increased monotonically with increasing Mn concentration (0.0-1.0) from 20.0 to 26.38 nm, respectively 14 as shown in Fig.3.

$$D = \frac{0.9\lambda}{\beta Cos\theta} \qquad ...(1)$$

X-ray wavelength, FWHM in radians and Bragg's angle, respectively, refer to λ, β, and θ. and dislocation density (δ) as

$$\delta = \frac{1}{D^2} \qquad ...(2)$$

Also, the larger ionic radius of Mn^{2+} compared to N^{2+} leads to stronger ionic interactions between them.[15] An increase in crystallite size typically results sharper and narrower peaks in an XRD pattern. This is because larger crystallites lead to a decrease in width of diffraction peaks, which enhances resolution of XRD pattern. So, for Mn doped nickel ferrites, sharp and crystalline peaks are observed after doping. The dislocation density decreases with increase in Mn concentration reveals that the less distortion in crystal lattice.

Fig.2: Enlarged preferred orientation peak for $Mn_xNi_{1-x}Fe_2O_4$ ferrite (x = 0.2, 0.4, 0.6,0.8, 1.0) nanoparticles

Scanning Electron Microscopy Study
The SEM micrographs for ferrite phase i.e. $Mn_xNi_{1-x}Fe_2O_4$ ferrite (x = 0.2, 0.4, 0.6,0.8, 1.0) composition is shown in Fig.4. The grains in the ferrite phase are smaller in size. The uniform nature of the particles is revealed with some agglomeration. The average grain size is about 97 nm. There is progress of grain size with calcination temperature. Increasing the Mn^{2+} ion concentration, the powder show irregular microstructures with small spherical particles and size of the particle is varied.[16] Generally, the grain size increases with an increase in Mn^{2+} ion concentration.

Optical analysis
UV-Visible Spectroscopy is used for the examination of the optical properties of Mn doped Ni ferrite nanoparticles. Solutions of Mn-Ni nano ferrites prepared by sonication in double distilled water were used to record the spectra. The absorption spectra were observed from 200nm to 800 nm as shown in figure Fig.5.

Fig.3: Crystallite size against Mn concentration for $Mn_xNi_{1-x}Fe_2O_4$ ferrite (x = 0.2, 0.4, 0.6, 0.8, 1.0) nanoparticles

**Table 1: Structural parameters for Mn$_x$ Ni$_{1-x}$Fe$_2$O$_4$ ferrite
(x = 0.2, 0.4, 0.6, 0.8, 1.0) nanoparticles**

Mn Concen-tration	Chemical Composition Mn$_x$ Ni$_{1-x}$Fe$_2$O$_4$	Average Crystallite Size (D) (nm)	Lattice parameter a (Å)	Average Dislocation Density (10^{16} lines/cm^2)
0	NiFe$_2$O$_4$	20.451	8.312	2.391
0.2	Mn$_{0.2}$ Ni$_{0.8}$Fe$_2$O$_4$	22.598	8.429	1.958
0.4	Mn$_{0.4}$ Ni$_{0.6}$Fe$_2$O$_4$	23.987	8.395	1.738
0.6	Mn$_{0.6}$ Ni$_{0.4}$Fe$_2$O$_4$	24.598	8.407	1.6353
0.8	Mn$_{0.8}$ Ni$_{0.2}$Fe$_2$O$_4$	25.985	8.421	1.481
1.0	MnFe$_2$O$_4$	26.987	4.459	1.373
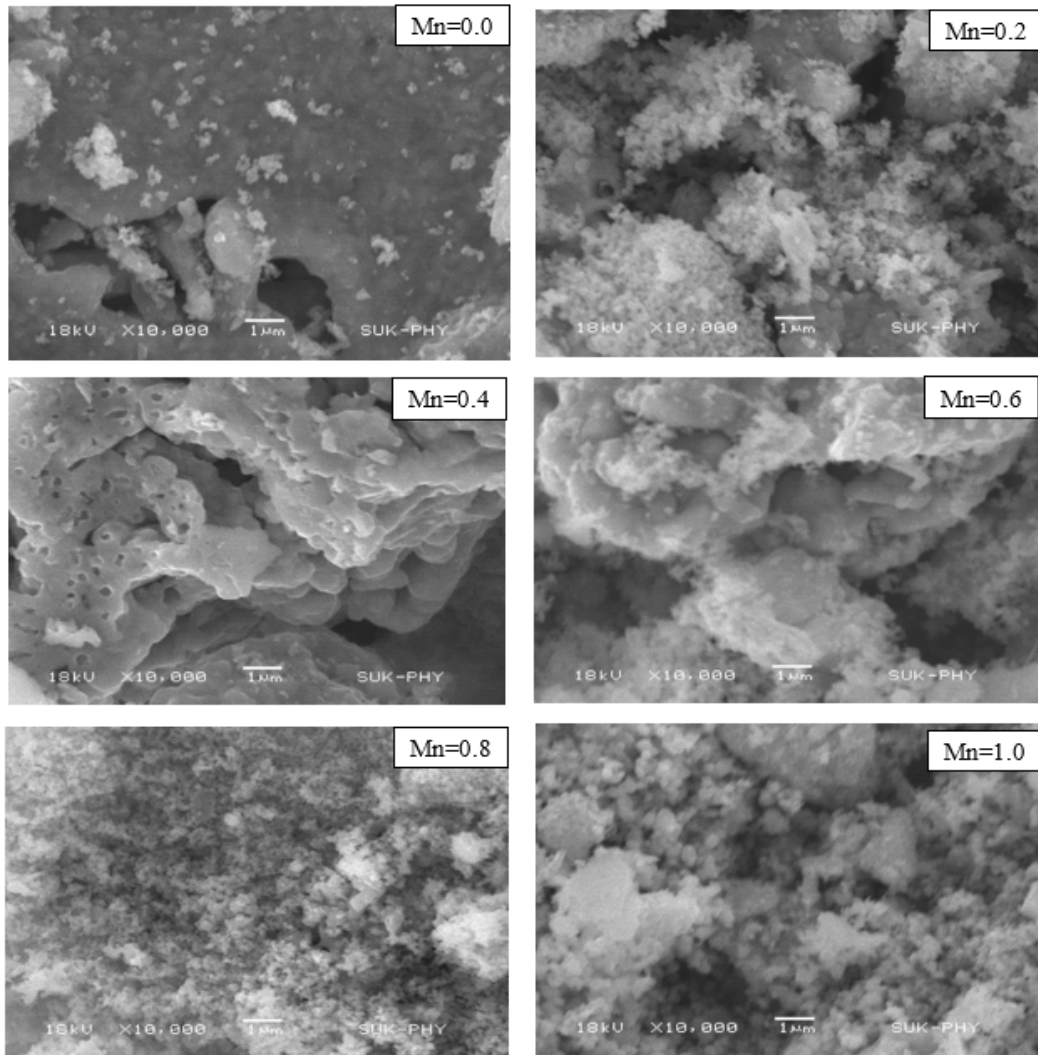
**Fig.4: Scanning Electron Micrographs for Mn$_x$ Ni$_{1-x}$Fe$_2$O$_4$ ferrite
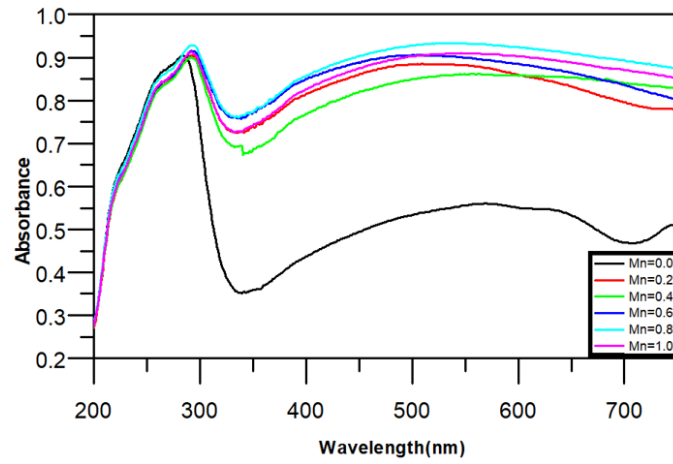(x = 0.2, 0.4, 0.6,0.8, 1.0) composition**

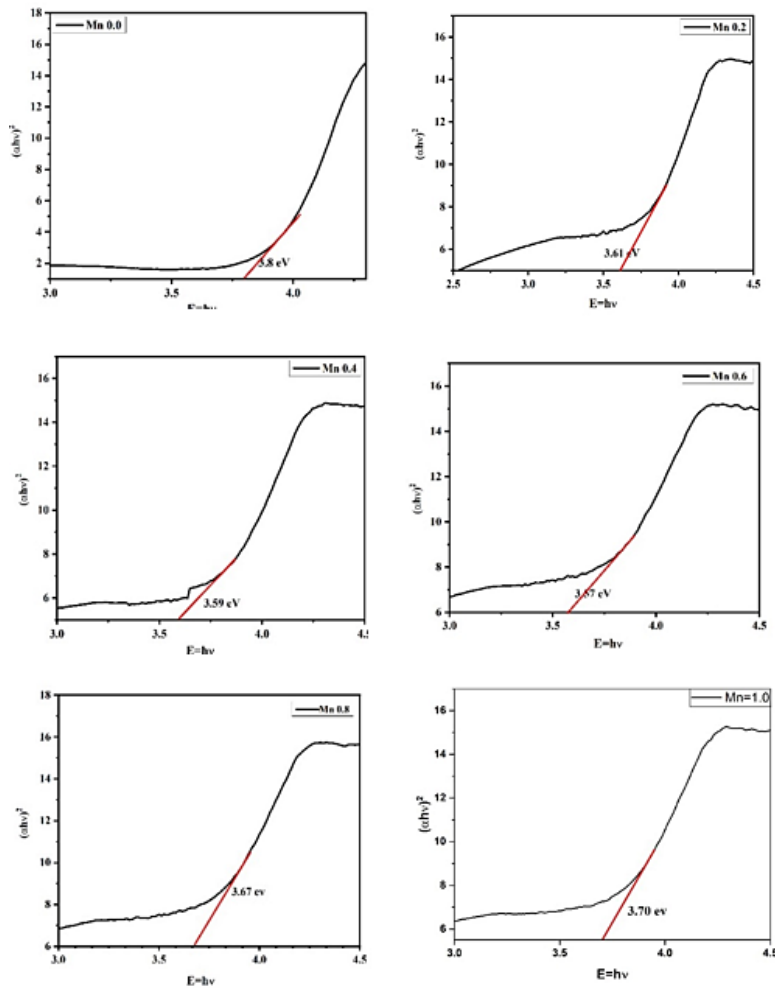**Fig.5: UV-Vis. spectra for Mn$_x$ Ni$_{1-x}$Fe$_2$O$_4$ ferrite (x = 0.2, 0.4, 0.6, 0.8, 1.0)**

Fig.6: Plot of (ahv)^2 against hv for the prepared Mn$_{0.0}$Ni$_{1.0}$Fe$_2$O$_4$ (x= 0.0, 0.2, 0.4, 0.6, 0.8, 1.0) nanoparticles

From absorption spectra, the variation in Mn composition in Ni ferrites causes the absorption change in the UV section about 300 nm (for $Mn_{0.8}Ni_{0.2}Fe_2O_4$) moves to longer wavelength visible region. This shifting to longer wavelength can be attributed to changes in electronic structure and composition of the material. Manganese doping alters the energy level and band structure, affecting absorption characteristics and again increase in absorption wavelength. To examine influence of Manganese effect on optical band gap, the Tauc equation is used for fitting absorption data.[17]

$$(\alpha h v)^n = C(h v - E_g) \qquad ...(1)$$

where C is proportionality constant, h is Planck constant, Eg is band gap, n is an integer which is '2' for direct band gap transition in present study and α is the absorption coefficient.

The plot of $(\alpha h v)^2$ with respect to energy of photon (hv) for all the Mn doped nickel nano ferrites are shown in Fig. 6. The extrapolation of the curve to the energy axis gives the band energy value for particular composition.

The values of band gap vary from 3.80 eV - 3.57 eV for Mn doped nickel ferrites. Thus, up to Mn=0.6 the projected value of band gap decreases is due to the quantum confinement effect. Further for Mn = 0.8 and 1.0 composition, the band gap rises may due to the little disorder in crystallinity of compositions. The increase in Mn produces additional energy levels in band structure. These levels can hybridize with existing energy bands of material, altering the band after Mn =0.8. Thus addition of Manganese for nickel ferrite leads to changes in electronic properties of materials in terms of tuned band gap, conductivity and absorption spectra.

Conclusions

Manganese doped nickel nanoparticles was synthesized by using self-propagating auto combustion method. The cubic spinel structure of Mn-Ni nanoparticles was identified by XRD. The agglomerated nature of ferrite particles nature is confirmed by Scanning electron Microscopy. The result indicate that the structural properties of nickel ferrite can be improved by Mn addition. The optical band gap for Mn- Ni nanoparticles decreases from 3.80 to 3.57 eV up to Mn = 0.6. The further rise of band gap only because of preparative crystallinity defects in composition revealed the variation of Mn in Ni ferrites for tuning its band gap. Thus variable narrow band gap can increase the efficiency of photo catalysis by enabling the absorption of a wide range of photons from solar spectrum and enhancing the generation of electron-hole pairs and facilitating more photocatalytic reactions.

References

1. Manikandan A, Vijaya JJ, Kennedy LJ, Bououdina M. "Structural optical and magnetic properties of Zn1-xCuxFe$_2$O$_4$ nanoparticles prepared by microwave combustion method", *J. Molecular Str*. 2013; 40: 1035:332

2. Gopalan E.V., Malini K.A., Sagar S, Kumar D.S., Yoshida Y, Al-Omari I.A, Anantharaman M.R. "Mechanism of ac conduction in nanostructured manganese zinc mixed ferrite", *J. Phys. D: Appl. Phys.,* 2009(16)

:165005

3. Devi E.C., Soibam I. "Effect of Zn doping on the structural, electrical and magnetic properties of MnFe$_2$O$_4$ nanoparticles". *Indian J. of Phys.,* 2017: 1-7

4. E. Ranjith kumar , R. Jayaprakash , M.S. Seehra , T. Prakash , Sanjay Kumar, "Effect of a-Fe $_2$ O$_3$ phase on structural, magnetic and dielectric properties of Mn–Zn ferrite nanoparticles" *J. Phys. Chem. Solid.:*2013:

74(7):943–949

5. Valenzuela R., "Novel applications of ferrites," *Physics Research International,* vol., Article ID 2012: 2012 (9) :591839

6. Latorre-Esteves M., Cortés A., Torres-Lugo M. and Rinaldi C., "Synthesis and characterization of carboxymethyl dextran-coated Mn/Zn ferrite for biomedical applications," *J. Magn. Mag. Mater,* 2009: 321(19) 3061–3066

7. A. Nigam and S. J. Pawar, "Structural, magnetic, and antimicrobial properties of zinc doped magnesium ferrite for drug delivery applications," *Ceram. Inter.* 2020: 46 (4) : 4058–4064

8. Kefeni K. K., Msagati T. A. M., Nkambule T. T. I. Mamba B. B., "Spinel ferrite nanoparticles and nanocomposites for biomedical applications and their toxicity," *Mater. Sci. Engin.*: C, 2020: 107: 110314

9. Javed F., Abbas M. A, Asad M. I. *et al.*, "Gd^{3+} doped $CoFe_2O_4$ nanoparticles for targeted drug delivery and magnetic resonance imaging," *Magnetochemistry,* 2021: 7 (4): 47

10. Ju W., Park J. H., Jung H. R., Cho S. J. and Lee W. J., "Electrospun $MnFe_2O_4$ nanofibers: preparation and morphology," *Comp. Sci. Techn.* 2008: 68 (7-8) : 1704–1709,

11. Maaz, K., Karim, S., Mumtaz, A., Hasanain, S.K., Liu J., Duan J.L., "Synthesis and magnetic characterization of nickel ferrite nanoparticles prepared by co-precipitation route", *Magn. Magn. Mat.* 2009: 321: 1838–1842

12. Hui, D.C., Xue, W.G., Lei, S., Wei, G.D., Jun, J.C., Sheng, X.D. "Investigation of the thermal stability of Mn ferrite particles synthesized by a modified co-precipitation method", Sci. *China Phys. Mech. Astron.* 2013:56(3): 568–572

13. Md. M. Roni, K. Hoque, A. C. Paul , M. N. I. Khan Synthesis of La-doped $Mn0·6Zn0.4LaxFe_2-xO_4$ and the study of its structural, electrical and magnetic properties for high frequency applications, *Results in Materials* 11:100215

14. P. Monisha , P. Priyadharshini , S.S. Gomathi , K. Pushpanathan, "Influence of Mn dopant on the crystallite size, optical and magnetic behaviour of $CoFe_2O_4$ magnetic nanoparticles", *J. Phys. Chem. Solid.,* 2021: 148: 109654

15. Gosh PK, Ahmed SF, Jana S, Chattopadhyay K.K., "Photoluminescence and field emission properties of ZnS:Mn nanoparticles synthesized by rf-magnetron sputtering technique", *Optical Mater.*, 2007 : (12) :1584-90.

16. Ranjith Kumar, E., Siva Prasada Reddy, P., Sarala Devi, G., Sathiyaraj, S.: Structural, dielectric and gas sensing behavior of Mn substituted spinel MFe_2O_4 (M = Zn, Cu, Ni, and Co) ferrite nanoparticles. *Magn. Magn. Mat.* 2016: 398, 281–288

17. Tahir, M.B., Iqbal, T., Hassan, A., Ghazal, S. "Wet chemical Coprecipitation synthesis of nickel ferrite nanoparticles and their characterization", *J. Inorg. Organomet. Polym. Mater.* 2017: 27, 1430– 1438.